

## Original Contributions

# Cholera Seasonality in Madras (1901–1940): Dual Role for Rainfall in Endemic and Epidemic Regions

Diego Ruiz-Moreno,<sup>1</sup> Mercedes Pascual,<sup>1</sup> Menno Bouma,<sup>2</sup> Andrew Dobson,<sup>3</sup> and Benjamin Cash<sup>4</sup>

<sup>1</sup>Department of Ecology and Evolutionary Biology, University of Michigan, 830 North University, 2041 Natural Science Building, Ann Arbor, Michigan, 48109-1048, USA

<sup>2</sup>Department of Infectious and Tropical Diseases, London School of Hygiene and Tropical Medicine, University of London, London, UK

<sup>3</sup>Department of Ecology and Evolutionary Biology, Princeton University, Princeton, New Jersey, USA

<sup>4</sup>Center for Ocean–Land–Atmosphere Studies, Calverton, USA

**Abstract:** The seasonality of cholera and its spatial variability remain unexplained. Uncovering the role of environmental drivers in these seasonal patterns is critical to understand temporal variability at longer time scales, including trends and interannual variability. Rainfall has been proposed as a key driver of the seasonality of cholera. To address this hypothesis, we examine the association between rainfall and cholera in both time and space using the extensive historical records for the districts of Madras in former British India (1901–1940). We show the existence of two main spatial clusters that differ not just in the effect of rainfall but also in the seasonal pattern and frequency of periods with and without cholera mortality. The results support a model of cholera seasonality with two different routes of transmission: one is enhanced by increasing rainfall (in areas with abundant water), the other is buffered by increasing water. We discuss how the dual nature of the influence of rainfall creates different temporal patterns in regions where cholera is either “endemic” or “epidemic.”

**Keywords:** Cholera, endemic cholera, epidemic cholera, rainfall

## INTRODUCTION

An understanding of the seasonality of cholera is still elusive despite the long history of descriptions of the patterns in different parts of the world and different regions of its center of endemism on the Indian sub-continent. Within regions, cholera cases can exhibit different seasonal patterns at different locations, including variations in the number of outbreaks and different delays with respect to peaks in rainfall and temperature. These patterns are not well

understood because environmental drivers themselves are poorly defined for the seasonal cycle of the disease. Two peaks per year is the typical pattern described for cholera in Bangladesh and former Bengal, with a decline in the summer during the monsoons, while only one peak coincident with the rainy season is present in other regions of former British India and contemporary Brazil (Codeco, 2001; Pascual et al., 2002). Despite these complexities, a better understanding of cholera’s seasonality is key to identify and understand the regional mechanisms behind the described influence of the El Niño Southern Oscillation (ENSO) (Pascual et al., 2000; Koelle and Pascual, 2004; Koelle et al., 2005b). It is also fundamental to build sce-

narios for cholera with global change. This is because both, climate variability (ENSO) and climate change, are likely to act on infectious disease dynamics through the modulation of the seasonal cycle and modification of the seasonal times when it crosses environmental thresholds (Pascual and Dobson, 2005).

The importance of rainfall as a driver of the seasonal cycle of cholera is implied by its waterborne transmission, the dose-dependent nature of infection, and the decline of cases during the monsoon season (Pascual et al., 2002). Rainfall as a driver is also intimately connected with the two routes of transmission described for cholera in the literature (Miller et al., 1985). Studies in volunteers have confirmed that ingestion of a dose between  $10^7$  and  $10^{11}$  is required to develop an infection (Kaper et al., 1995). Brackish waters and estuaries provide suitable environmental conditions for the bacterium to survive outside the human host (Colwell et al., 1977). In these aquatic free-living environments, both pathogenic and non-pathogenic *V. cholerae* survive in free-living states as well as attached to invertebrates and algae in the plankton (Colwell, 1996; Islam et al., 2004). Thus, primary transmission presumably occurs from a reservoir of the pathogen, *V. cholerae*, in the aquatic environment. A more direct transmission route, known as secondary or “human-to-human” transmission, is mediated by the ingestion of fecally contaminated water or food (Miller et al., 1985; Glass et al., 1991). The relative importance of these two routes of transmission has been highly debated since early times when “contagionists” emphasized the role of human contact while “localists” focused on geography and the environment (Pascual et al., 2002). The importance of “human-to-human” transmission is supported by recent time series models fitted to the endemic dynamics of cholera in Bangladesh (Koelle and Pascual, 2004; Koelle et al., 2005b). In these, there is a clear feedback between present and past levels of infection in the population. The existence of a short-lived hyper-infective stage provides one mechanism enhancing this transmission route (Merrell et al., 2002; Hartley et al., 2006). Clearly, the categorization of the two transmission pathways is a simplification that considers the two extremes of a continuum defined by the strength of the feedback between past and future cases and by different temporal scales of transmission (Pascual et al., 2006). For primary transmission, this feedback is weak (in the extreme nonexistent), predominantly because the bacterium concentration in the environment is dominated by stochastic environmental drivers that influence its survival and population growth. However,

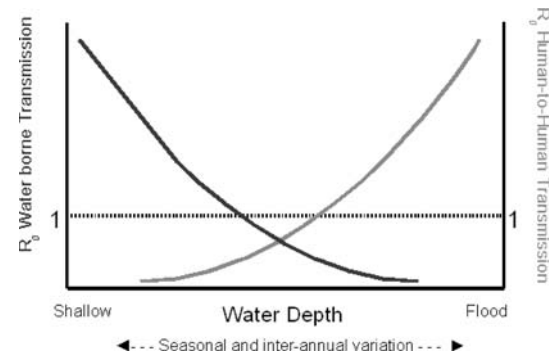


**Figure 1.** Graphical model showing the influence of water depth on the two routes of transmission proposed for cholera. Outbreaks occur when  $R_0 > 1$ . The dark gray line shows the decrease of primary transmission as water depth increases, while the gray line shows the increase of secondary transmission. Under shallow-water conditions, primary transmission is high, while flood conditions turn on and favor the subsequent development of secondary transmission.

at the other extreme of almost direct “human-to-human” transmission, the feedback is strong, whether or not transmission occurs through water in the environment, and the transmission rate is a function of the level of infection in the population.

Based on these two transmission routes, Dobson et al. [in preparation] have proposed the following mechanisms behind the bimodal seasonal pattern of cholera in Bangladesh. The first peak occurs in the spring, during the dry season when temperature warms up, because the bacterium thrives in the environment where it is also highly concentrated and human interactions with the limited water bodies available in the environment increase (i.e., strong primary transmission). The monsoons then lead to a decline in cholera in the summer, as heavy rainfall dilutes the concentration of the pathogen in the environment and favorable conditions of salinity and pH deteriorate. This dilution effect of rainfall represents a negative influence. However, a positive delayed effect would also occur, leading to an increase in cholera, when humans concentrate in the flooded landscape and the existing sanitary conditions break down exacerbating secondary transmission (see Fig. 1) or when the free-living stages escape the influence of the phages that may play a major role in regulating their abundance (Faruque et al., 2005).

This seasonal model provides predictions for both endemic and epidemic areas. In endemic regions, cholera should exhibit a negative association with rainfall at zero lag, largely reflecting the dilution effect, and a positive correlation at positive lags reflecting the increase in secondary transmission after the rains. However, in regions

with long and sustained periods of rainfall, and consequently with low concentration of the pathogen in aquatic reservoirs, the local extinction of the disease should be more likely. Hence, frequent fade-outs and more irregular temporal patterns should be favored in regions with sustained rainfall and lower human populations. To examine these predictions, we analyze the association of cholera and rainfall in space and time, investigating also the notion of a Critical Community Size, the existence of a population threshold for disease persistence (Bartlett, 1957; Keeling, 1997).

The historical records for cholera mortality in the districts of former British India provide an opportunity to consider extensive temporal records across geographical regions. We focus here on the districts of the Madras Presidency, as cholera and climate data for this region span both a large region of historic and present day India; they exhibit a range of seasonal cholera patterns, from regular to irregular, with one or two peaks per year. Based on cholera-rainfall associations and fade-out patterns, we describe two main district clusters corresponding, respectively, to “epidemic” and “endemic” regions, and with distinct roles of rainfall. We provide evidence for the proposed positive and negative effects of rainfall in the bimodal seasonal cycle of endemic cholera. The spatio-temporal patterns of cholera mortality suggest a complex role of this environmental variable in the dynamics of the disease.

## METHODS AND DATA

The area studied corresponds to the region of former British India known as the Madras Presidency. The Madras Presidency included several districts in the southern region of India between latitudes  $20^{\circ}$  and  $8^{\circ}$ N and longitudes  $74^{\circ}$  and  $86^{\circ}$ E. We digitized the historical maps of the province and its 26 administrative sub-province divisions or districts (Fig. 2).

For each district, monthly cholera mortality data were extracted from the records (*Annual Yearbooks of the Sanitary Commissioner, Madras*, printed by the Superintendent, Government Press, Madras) from January 1892 to December 1940 and, for the same period, population sizes were obtained (from census every 10 years). In addition, from January 1901 to December 1970, several meteorological stations located in the region recorded daily rainfall data (Table 1). We produced a monthly estimate of rainfall

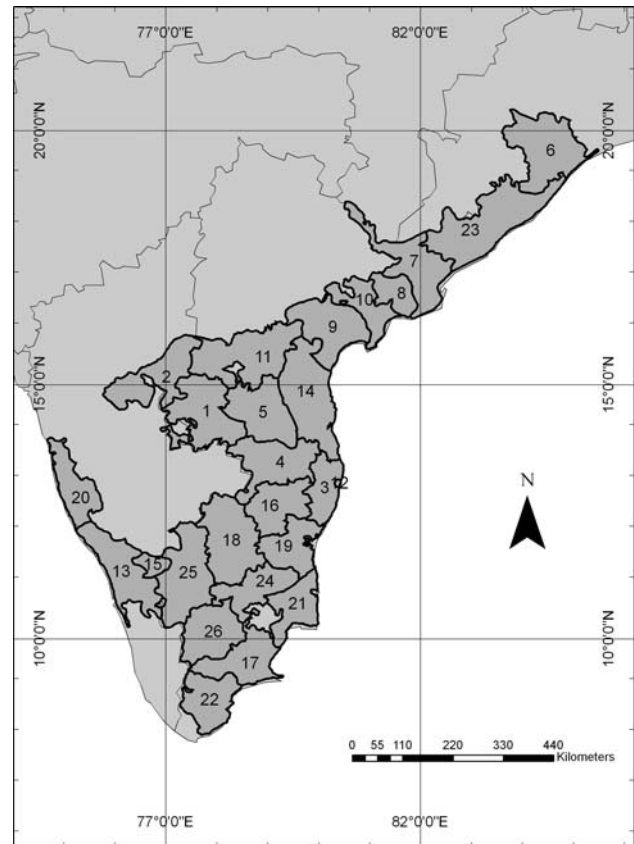


**Figure 2.** The Madras Presidency with its 26 districts: (1) Anantapur; (2) Bellary; (3) Chingleput; (4) Chittoor; (5) Cuddapah; (6) Ganjam; (7) Godivari East; (8) Godivari West; (9) Guntur; (10) Kistna; (11) Kurnool; (12) neighborhood of Madras, the former capital city; (13) Malabar; (14) Nellore; (15) Nilgiris; (16) North Arcot; (17) Ramnad; (18) Salem; (19) South Arcot; (20) South Kanara; (21) Tanjore; (22) Tinnevely; (23) Vizagapatam; (24) Trichinopoly; (25) Coimbatore; and (26) Madua.

per district by averaging the readings of the corresponding meteorological stations while taking into consideration the historical borders of the districts. Because of the partial temporal overlap of the records, analyses requiring both datasets only included the period from January 1901 to December 1940. On the other hand, whenever cholera mortality or rainfall were analyzed independently, the full extent of the time series was used (1892–1940 and 1901–1970, respectively).

A spatial correlogram (Bailey and Gatrell, 1995; Fortin et al., 2002), for mean cholera mortality for each district and the distance between their centroids was performed to define the distance for which the disease autocorrelation decays to zero. This distance allows us to define districts that are considered neighbors and are specified as such in a proximity matrix. We used this proximity matrix to

**Table 1.** Number of Meteorological Stations per District<sup>a</sup>

District	No. of meteorological stations
Anantapur	10
Bellary	9
Chingleput	11
Chittoor	8
Cuddapah	10
Ganjam	12
Godivari East	18
Godivari West	5
Guntur	15
Kistna	9
Kurnool	9
Madras	—
Malabar	23
Nellore	14
Nilgiris	9
North Arcot	11
Ramnad	9
Salem	21
South Arcot	13
South Kanara	10
Tanjore	17
Tinnevely	8
Vizagapatam	21
Trichinopoly	17
Coimbatore	15
Madua	10

<sup>a</sup>The rainfall data of Chingleput were used for the city of Madras.

examine the spatial structure of the association between cholera and rainfall. The coefficient of cross-correlation between the cholera and rainfall time series was calculated for lags ranging from 0 to 12 months (with rainfall preceding cholera). We applied the well-known (global) autocorrelation index, Moran's I (Cliff and Ord, 1973) to this quantity to determine the degree of clustering of the association between cholera and rainfall. To further determine the geographical location of the clusters, we applied the modification of the Moran's index known as the Local Indicator of Spatial Association, LISA (Anselin, 1995). Whereas Moran's I evaluates the degree of global clustering, the LISA index allows for local variation and therefore localizes "hot-spots" and "cold-spots," or clusters, with respectively high and low associations values between cholera and rainfall. To determine whether clusters in the

association reflect the spatial structure of the disease itself, we applied these same indices to the mean cholera mortality per district.

The spatio-temporal dynamics of cholera mortality and the degree of spatial association can also be analyzed by looking at the synchrony of outbreaks in the Madras Presidency. Synchrony between populations can be quantified with the zero-lag-cross-correlation between the time series of log-cases evaluated against the region-wide synchrony (Bjornstad et al., 1999a). To calculate the zero-lag-cross-correlation, we first define a new time series,  $z_t$ , which corresponds to the first-differenced time series of log-transformed cholera mortality (i.e.,  $z_t = \log(N_t + 1) - \log(N_{t-1} + 1)$ ; where a 1 has been added to handle the case of no reported deaths). The average of the cross-correlation coefficient, which is known as the region-wide synchrony, is defined as

$$\text{average}(\rho_{i,j}) = \frac{2}{N \cdot (N - 1)} \cdot \sum_{i=1}^N \sum_{j=i+1}^N \rho_{i,j}$$

where  $\rho_{i,j}$  represents the cross-correlation coefficient between the time series  $z_t$  at sites  $i$  and  $j$ . Because the cross-correlation coefficients are not independent, a bootstrap confidence interval for the mean synchrony was generated using a sampling method (Bjornstad et al., 1999b). The same analysis was applied to the rainfall data to examine whether patterns of synchrony correspond to those of rainfall.

Besides the existence of an association with rainfall, our hypothesis on cholera seasonality predicts that different patterns of disease persistence should be observed in districts with different intensity of the rainfall season. To examine this prediction, two dynamical measures were considered: the Critical Community Size and the seasonal variability of rainfall. The Critical Community Size (CCS), the population size below which a disease dies out in the troughs between epidemics, reflects the dynamics of extinction (Keeling, 1997). Hence, a qualitative measure of the CCS was obtained for the districts where population data were available. A period of at least two consecutive months without mortality was considered a "fade-out." The same qualitative results were obtained when this analysis was performed with longer and shorter periods (ranging from 1 to 6 months for the definition of a fade-out).

Rainfall patterns were first examined by themselves, and then in association with cholera cases. All the districts exhibited a high annual peak in rainfall due to the

southwest monsoon (Krishnamurthy and Kinter, 2002). When the mean and the variance of rainfall were compared among districts, no statistically significant differences were found (results not shown). However, some districts exhibited high precipitation values lasting up to 6 months, with negligible precipitation during the rest of the year, whereas other districts had shorter monsoon seasons of 3–4 months with a second peak of rainfall later in the year. Exceptions without this second peak are found in the districts on the Arabian Sea. Therefore, in these analyses, we focused on the length of the rainy season. By determining how many times and for how long the monthly accumulated rainfall exceeded a threshold value—fixed at a value of 25% above the district mean—we discriminated districts with two rainfall peaks per year from those with only one. We used this classification to interpret the clustering patterns arising from the rainfall–cholera associations. Consideration of other threshold values (between 25% and 75% above the district rainfall mean) led to similar conclusions.

## RESULTS

The dynamics of the disease and its seasonal cycle appear to differ across the districts. Some districts exhibit intermittent epidemics with numerous fade-outs, while others display seasonal outbreaks every year with high persistence of the disease. Two peaks per year are typically seen in the latter, while a single peak is present for the more irregular patterns. In addition, these seasonal patterns also differ in their typical lags relative to rainfall. Figure 3 illustrates these patterns for two representative districts. To better understand and characterize the spatio-temporal patterns of the disease, as well as their relationship to rainfall, we begin by considering the existence of district clusters for both rainfall and cholera independently, and for their association.

Based on the result of the spatial correlogram, districts within 200 Km or less were considered as neighbors (Fig. 4). The values obtained for the spatial autocorrelation, measured by the global index Moran's I, indicate that there is no significant spatial clustering when both cholera mortality and rainfall are independently considered (Table 2). However, this index becomes significant when evaluated for the cross-correlation between these variables, providing evidence for a spatial association between cholera and rainfall (Table 2).

Similarly, only small clusters emerged from the analysis of the independent variables with the LISA index, while two distinct larger clusters are apparent for their cross-correlation. Specifically, the LISA index for cholera mortality delimited one small-size cluster (districts number 17, 24, and 26) with high values in the central southern part of the region under analysis, and a second cluster close to the first, also small in size (districts 15 and 18) with low values. For rainfall, a medium-size cluster (districts number 4, 5, 11, and 14) of low values appears in the central northern region. More interestingly, when the cross-correlation between cholera and rainfall at zero lag is considered, one large cluster emerges in the northeast region for positive significant correlations (including districts 7, 8, 9, 10, 11, and 23, and denoted as *positive correlation cluster* in Fig. 5). A second large cluster with negative significant values is found in the central southern area (including districts 15, 16, 17, 18, 19, 21, 24, 25, and 26, and denoted as *negative correlation cluster* in Fig. 5). When time lags are introduced for 3–7 months, the main pattern is reversed: the cluster in the southern region now reflects positive associations, while the northern one exhibits negative ones (Fig. 6). As expected for a seasonal pattern, the same clustering patterns emerge for lags close to 12 months.

These results are corroborated by the ones on the synchrony of outbreaks. Very low synchrony is observed when both cholera and rainfall are considered separately, with only a few districts with significant zero-lag-cross-correlation values (results not shown). The lack of synchrony is consistent with the existence of two different clusters (the positive correlation cluster and the negative correlation cluster) for the association between cholera and rainfall.

We examined next whether the districts, for the different clusters we have identified, exhibit different dynamic patterns of disease persistence. As expected from theoretical considerations with stochastic disease models (Bartlett, 1957; Keeling, 1997), patterns of persistence are influenced by population size. Figure 7 shows that districts with a higher density have a lower number of fade-outs, while those with a lower density experience more frequent fade-outs. This implies that cholera is endemic and exhibits more regular seasonality in districts with higher population densities, while outbreaks are epidemic and highly intermittent in those with lower densities. A chi-squared test comparing the distributions for the number of fade-outs between low and high density districts establishes that the differences between these districts are statistically signifi-

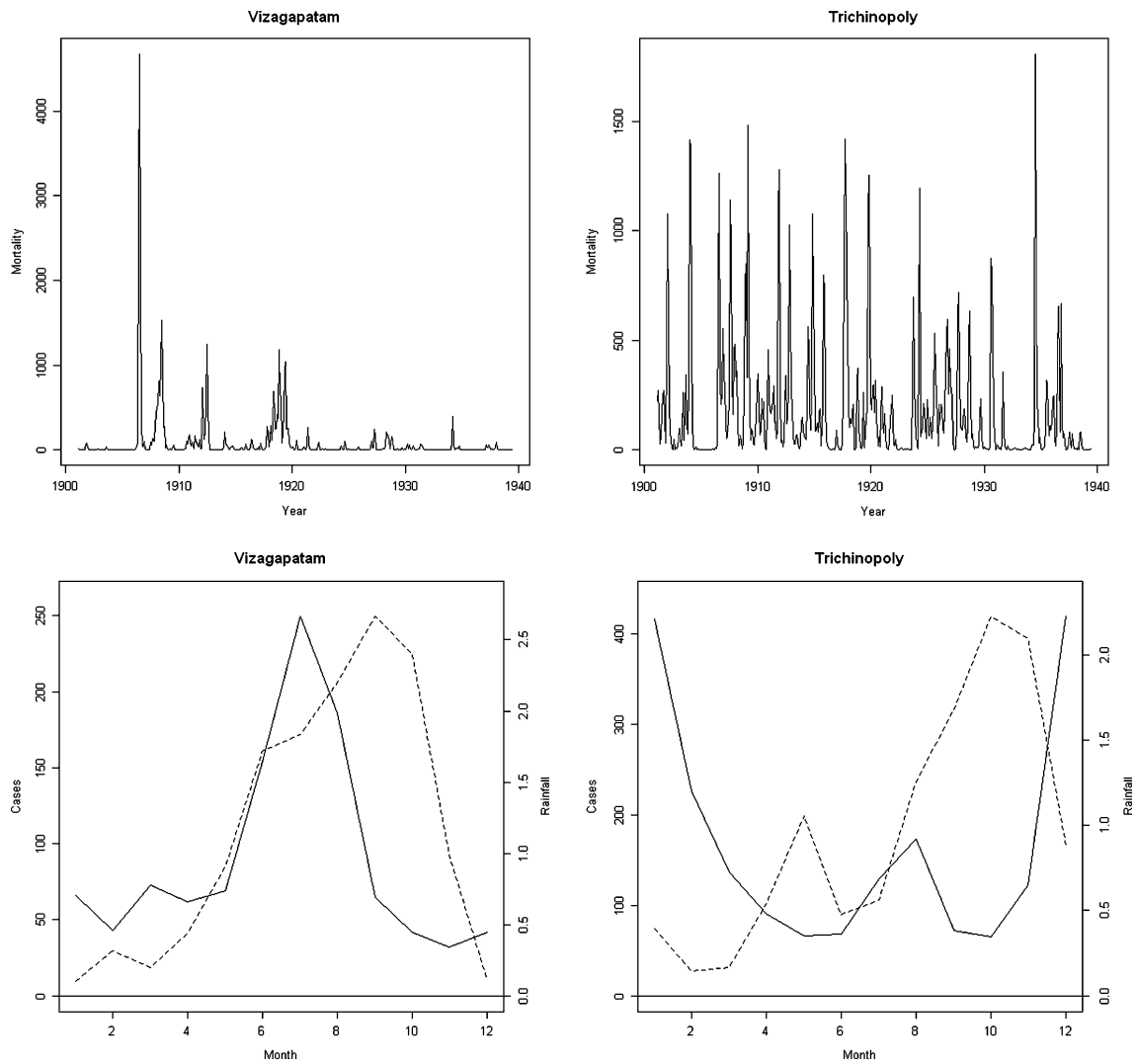


**Figure 3.** The upper panels show monthly cholera mortality from 1901 to 1940 for two representative districts for the two regions identified in this work: Vizagapatam (top, left) illustrates the intermittent epidemic patterns observed in the northeast region; while Trichinopoly (top, right) exhibits the more regular seasonal pattern characteristic of endemic dynamics. The bottom panels show, for these same two districts, the monthly averages for rainfall (dotted lines) and cholera mortality (solid lines). In Vizagapatam (bottom, left), one long rainy season typically coincides with cholera outbreaks in years when disease is present; in Trichinopoly (bottom, right), two distinct rainy periods can be recognized that are typically out of phase with the two cholera mortality peaks.

cant (Kruskal-Wallis  $\chi^2 = 6$ ,  $P$ -value = 0.01; low and high density districts are defined as those with densities between 45 and 65.7 h/Km<sup>2</sup> and 164 and 201 h/Km<sup>2</sup>, respectively).

To determine whether fade-out patterns have a spatial structure, we compared the distribution of the number of fade-outs between northern and southern districts. The “per year” mean (total number of fade-outs divided by the length of the time series in years) in the northern districts (1.985) is significantly larger than the one for the southern districts (0.785) (Kruskal-Wallis  $\chi^2 = 5.4857$ ,  $P$ -value = 0.01, Fig. 8). A similar geographical pattern is obtained for

the distribution of the duration of fade-outs, with the northern districts exhibiting longer fade-outs than the southern ones (Kruskal-Wallis  $\chi^2 = 9$ ,  $P$ -value = 0.0027).

Do these two regions with different fade-out patterns correspond to different durations of the rainfall season? Based on the distribution of the annual duration of the rainy season, we distinguished three different regions (Fig. 8): a northern area with a long season (districts 6, 7, 8, 9, 10, 13, 15, 20, and 23, with an average length of 4.04 months); a central area with rains of moderate length (districts 1, 2, 3, 4, 5, 11, 12, 14, 16, 19, and 21, with an

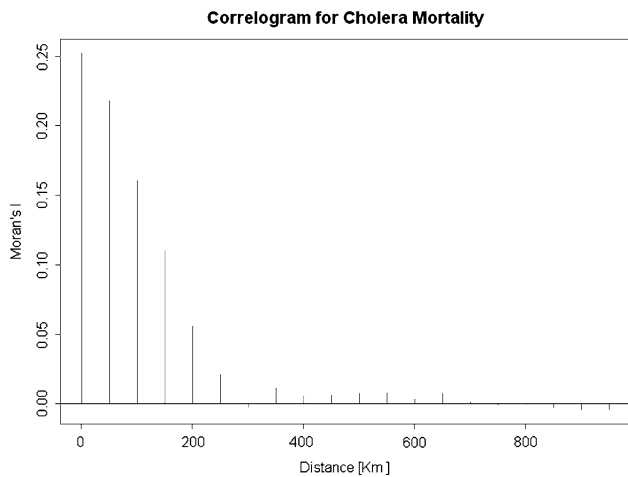


**Figure 4.** Spatial correlogram for cholera mortality in Madras computed from the mean value of cholera mortality per district and the distance between the districts’ centroids. The value of the Moran’s index indicates the influence of mortality across districts for a given distance. The distance of 200 Km was selected as the boundary defining districts as “neighbors.”

**Table 2.** Moran’s Index for the Different Variables\*

	Mean cholera	Mean rainfall	Cross-correlation between cholera and rainfall
Moran’s I	0.05 (0.187)	0.15 (0.018)	0.49 (0.001)

\*The *P*-values are indicated in parentheses.

average length of 2.82 months); and a southern region with two shorter wet seasons (districts 17, 18, 22, 24, 25, and 26, with an average length of 2.3 months). These three regions are statistically different for the length of the rainy season (Kruskal-Wallis  $\chi^2 = 14.1429$ , *P*-value = 0.0001694 for the comparison of regions with long and moderate rainy seasons; Kruskal-Wallis  $\chi^2 = 10.125$ , *P*-value = 0.001463 for regions with long and short rainy seasons; and Kruskal-Wallis  $\chi^2 = 7.1021$ , *P*-value = 0.007699 for regions with moderate and shorter seasons).

## DISCUSSION

The above results split the Madras Presidency into two main regions with different seasonal patterns of rainfall and cholera dynamics. The southern region exhibits a seasonal

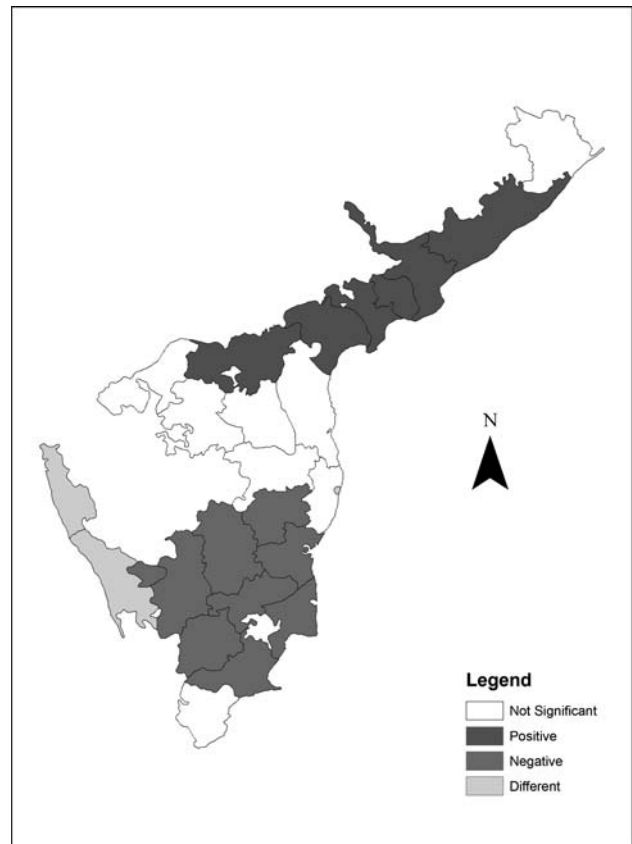


**Figure 5.** The LISA index applied to the coefficient of cross-correlation between cholera and rainfall (for zero lag). A cluster of positive correlation values between rainfall and cholera mortality is observed in the northeast region, while a cluster exhibiting negative correlation values is present in the south. Three districts show a statistically different pattern from the districts defined as neighbors (presenting positive correlation values when their neighbors exhibit a negative value or vice versa). All clusters are statistically significant with *P* < 0.05 for 999 random realizations.

disease pattern similar to the one described in the literature for former Bengal and Bangladesh (Bouma and Pascual, 2001; Koelle et al., 2005a), with two peaks per year; there is, however, a shift in the timing of the outbreaks consistent with the earlier dominant monsoon season. This seasonal pattern is then characteristic of “endemic” regions, with regular and persistent infection, and contrasts with the more stochastic nature of “epidemic” regions, with recurrent fade-outs and only one sporadic peak coincident with the rains. These patterns in Madras can be taken as a basis to consider the seasonal patterns of cholera in other regions, including those where the disease is a public health burden today. Endemic cycles have been described for historical data in former Bengal, while epidemic patterns occurred in the dryer region of former Punjab (Pascual

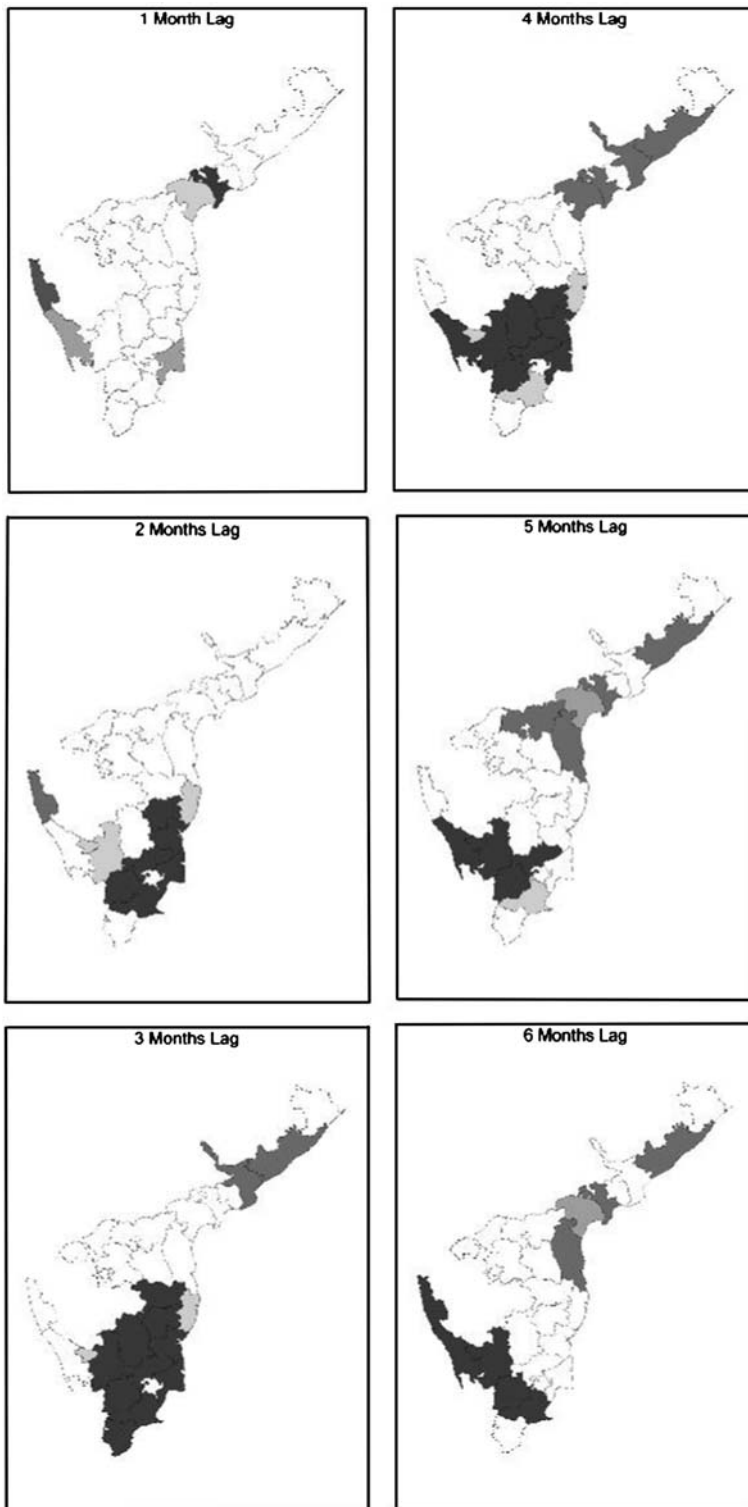


**Figure 6.** The LISA index applied to the coefficient of cross-correlation between cholera and rainfall for different time lags (with cholera behind rainfall). The color-coding is the same as shown on Figure 5. All clusters are statistically significant with  $P < 0.05$  for 999 random realizations.

et al., 2002). Epidemic cycles with significant fade-outs occur in coastal regions of western Africa today (Lan and Reeves, 2002). Their seasonal relationship to rainfall patterns remains to be examined and compared to our findings here.

In the southern region of Madras, fade-outs are short and infrequent, indicating a more permanent presence of the disease and the pathogen (Fig. 3). A negative association between cholera and rainfall is observed at zero lags reflecting the consistent decline of cases during the mon-

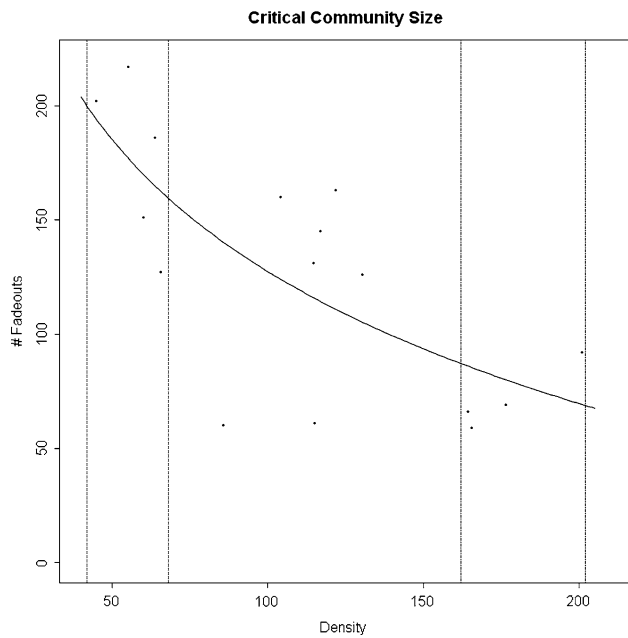


**Figure 7.** Critical Community Size, showing the number of fade-outs for the different districts against their population density [h/Km<sup>2</sup>]. The (logarithmic) fitted curve ( $R^2 = 0.5157$ ) illustrates the general decreasing trend in the number of fade-outs as density increases. The values obtained for the spatial autocorrelation, measured by the global index Moran's I, indicate that there is neither significant spatial clustering for the number of fade-outs (Moran's I = 0.14,  $P$ -value = 0.08 for 999 random realizations) nor for the population density (Moran's I = 0.17,  $P$ -value = 0.06 for 999 random realizations). The low-density districts (between the vertical dashed lines on the left) exhibit irregular outbreaks, while those with higher population density (between the dot-dashed lines on the right) exhibit a regular seasonal pattern.

soons, in between the two peaks. For the same region, the reversal to a positive association reflects the increase in cases that follow the monsoons. These results for the southern pattern are consistent with the predictions of our seasonal model, with a “dilution” effect of rainfall on the environmental concentration of the pathogen but also an enhancing effect on secondary transmission during extreme rainfall events [Dobson et al., in preparation]. While the first effect has been described in the literature, the second is novel for the bimodal cholera pattern.

The northeast cluster, defined by a positive correlation with rainfall at zero lag, is mainly composed of districts with a single epidemic peak when present. These districts display longer and more frequent fade-outs (Fig. 3). This unimodal pattern coincident with the monsoons combined with its stochastic nature suggests that in places where secondary transmission cannot be sustained over time, an

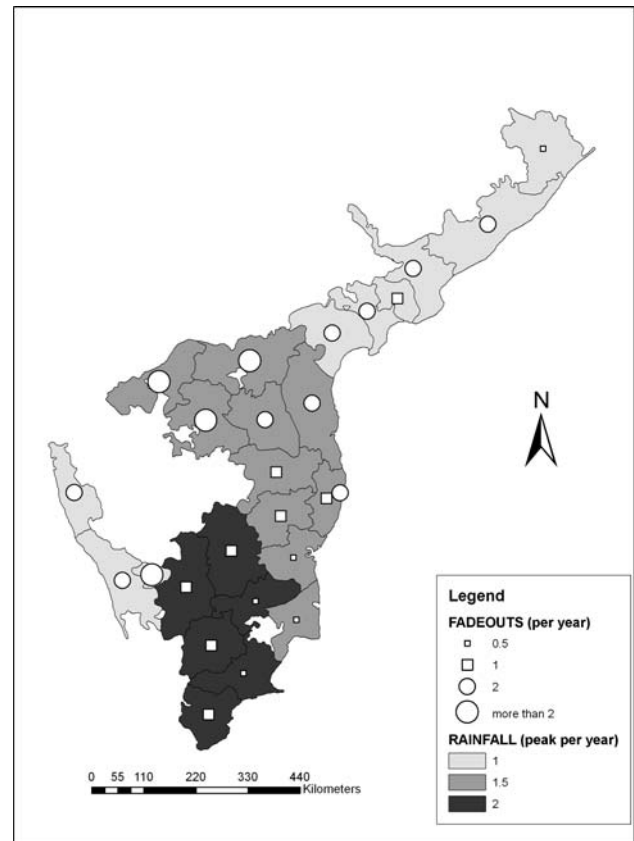


**Figure 8.** The spatial distribution of the average number of fade-outs and rainfall peaks per year. Districts with one and two peaks per year exhibit short and long rainy seasons, respectively. The districts on the Arabian Sea (13, 15, and 20 in Fig. 2) do not follow this pattern.

environmental reservoir of pathogenic *Vibrio cholerae* is not effectively maintained at a level sufficient to cause disease. More sustained periods of rain imply longer duration of the dilution of the pathogen concentration in aquatic reservoirs, and epidemics occur during the rainy season presumably through immigration of infected individuals and the consequent secondary route of transmission. In endemic regions, the human feedback from infected individuals to aquatic reservoirs appears critical to sustain the so-called primary transmission.

These results underscore the complexities of the role of rainfall on the seasonal dynamics of cholera, and their dependency on the endemic vs. epidemic nature of the disease. Open questions remain on the mechanisms behind the different lags in different regions for the positive effect of rainfall on transmission. A better understanding of these different lags will require a more detailed analysis of the spatio-temporal patterns focused on the spatial propagation

of the disease. In particular, mechanistic models should examine how the persistence of an environmental reservoir interacts with levels of immunity in the population in ways that may affect disease dynamics at seasonal scales. The effect of environmental water levels on the recently discovered interaction between the *V. cholerae* and phage (Faruque et al., 2005) must also be examined [Dobson et al., in preparation]. Both these mechanisms could affect the lag of cholera outbreaks relative to the timing of rainfall events.

The existence of both positive and negative effects of rainfall in the seasonal cycle is consistent with the previously described associations of this variable with the transmission rate of cholera at longer temporal scales. Recent findings suggest that high precipitation and flooding mediate, in part, the effect of El Niño in the approximately 4-year cycle of the disease (Koelle et al., 2005b). The same time series model indicates, however, that at even longer temporal scales, rainfall and river discharge are negatively associated with disease transmission. The complex role of water reflects multiple mechanisms and spatio-temporal scales involved in the concentration of the pathogen in the environment and in the human behavior underlying contact with water and the pathogen itself. The seasonal model supported by these findings can be used to further investigate these mechanisms and provides a basis to build predictive models that incorporate seasonality as a function of environmental drivers.

## ACKNOWLEDGMENTS

We thank two anonymous reviewers for their comments. This work was supported by the National Science Foundation–National Institutes of Health (Ecology of Infectious Diseases Grant EF 0430 120) and the National Oceanic and Atmospheric Administration (Oceans and Health Grant NA 040 AR 460019).

## REFERENCES

- Anselin L (1995) Local indicators of spatial association—LISA. *Geographical Analysis* 27:93–115
- Bailey TC, Gatrell AC (1995) *Interactive Spatial Data Analysis*, Harlow, UK/New York: Longman Scientific & Technical. New York: John Wiley & Sons
- Bartlett MS (1957) Measles periodicity and community size. *Journal of The Royal Statistical Society Series A—General* 120:48–70
- Bjornstad ON, Ims RA, Lambin X (1999a) Spatial population dynamics: analyzing patterns and processes of population synchrony. *Trends in Ecology & Evolution* 14:427–432
- Bjornstad ON, Stenseth NC, Saitoh T (1999b) Synchrony and scaling in dynamics of voles and mice in northern Japan. *Ecology* 80:622–637
- Bouma M J, Pascual M (2001) Seasonal and interannual cycles of endemic cholera in Bengal 1891–1940 in relation to climate and geography. *Hydrobiologia* 460:147–156
- Cliff AD, Ord JK (1973) *Spatial Autocorrelation*. London: Pion
- Codeco CT (2001) Endemic and epidemic dynamics of cholera: the role of the aquatic reservoir. *BMC Infectious Diseases* 1:1
- Colwell RR (1996) Global climate and infectious disease: the cholera paradigm. *Science* 274:2025–2031
- Colwell RR, Kaper J, Joseph W (1977) Vibrio-cholerae, Vibrio-parahaemolyticus, and other Vibrios—occurrence and distribution in Chesapeake Bay. *Science* 198:394–396
- Faruque SM, Bin Naser I, Islam MJ, Faruque ASG, Ghosh AN, Nair GB, et al. (2005) Seasonal epidemics of cholera inversely correlate with the prevalence of environmental cholera phages. *Proceedings of the National Academy of Sciences of the United States of America* 102:1702–1707
- Fortin M-J, Dale MRT, ver Hoef J (2002) Spatial analysis in ecology. In: *Encyclopedia of Environmetrics, Vol 4*, El-Shaarawi AH, Piegorors WW (editors), Chichester, UK: John Wiley & Sons, pp 2051–2058
- Glass RI, Claeson M, Blake PA, Waldman RJ, Pierce NF (1991) Cholera in Africa—lessons on transmission and control for Latin-America. *Lancet* 338:791–795
- Hartley DM, Morris JG, Smith DL (2006) Hyperinfectivity: a critical element in the ability of *V. cholerae* to cause epidemics? *PLoS Medicine* 3:63–69
- Islam MS, Mahmuda S, Morshed MG, Bakht HBM, Khan MNH, Sack RB, et al. (2004) Role of cyanobacteria in the persistence of *Vibrio cholerae* O139 in saline microcosms. *Canadian Journal of Microbiology* 50:127–131
- Kaper JB, Morris JG, Levine MM (1995) Cholera. *Clinical Microbiology Reviews* 8:48–86
- Keeling MJ (1997) Modelling the persistence of measles. *Trends in Microbiology* 5:513–518
- Koelle K, Pascual M (2004) Disentangling extrinsic from intrinsic factors in disease dynamics: a nonlinear time series approach with an application to cholera. *American Naturalist* 163:901–913
- Koelle K, Pascual M, Yunus M (2005a) Pathogen adaptation to seasonal forcing and climate change. *Proceedings of the Royal Society of London. Series B: Biological Sciences* 272:971–977
- Koelle K, Rodo X, Pascual M, Yunus M, Mostafa G (2005b) Refractory periods and climate forcing in cholera dynamics. *Nature* 436:696–700
- Krishnamurthy V, Kinter JL III (2003) The Indian monsoon and its relation to global climate variability. In: *Global Climate: Current Research and Uncertainties in the Climate System*, 286 pp, Rodó X, Comín F (editors), Berlin: Springer-Verlag, pp 186–236
- Lan RT, Reeves PR (2002) Pandemic spread of cholera: genetic diversity and relationships within the seventh pandemic clone of *Vibrio cholerae* determined by amplified fragment length polymorphism. *Journal of Clinical Microbiology* 40: 172–181

- Merrell DS, Butler SM, Qadri F, Dolganov NA, Alam A, Cohen MB, et al. (2002) Host-induced epidemic spread of the cholera bacterium. *Nature* 417:642–645
- Miller CJ, Feachem RG, Drasar BS (1985) Cholera epidemiology in developed and developing-countries—new thoughts on transmission, seasonality, and control. *Lancet* 1:261–263
- Pascual M, Dobson A (2005) Seasonal patterns of infectious diseases. *PLoS Medicine* 2:18–20
- Pascual M, Bouma MJ, Dobson AP (2002) Cholera and climate: revisiting the quantitative evidence. *Microbes and Infection* 4:237–245
- Pascual M, Koelle K, Dobson AP (2006) Hyperinfectivity in cholera: a new mechanism for an old epidemiological model? *PLoS Medicine* 3(6): e280. DOI 10.1371/journal.pmed.0030280
- Pascual M, Rodo X, Ellner SP, Colwell R, Bouma MJ (2000) Cholera dynamics and El Niño-Southern Oscillation. *Science* 289:1766–1769